

## Crowded, Confined, and Frustrated: Dynamics of Molecules Tethered to Nanoparticles

Praveen Agarwal, Sung A. Kim, and Lynden A. Archer

*Chemical and Biomolecular Engineering, Cornell University, Ithaca, New York 14850, USA*

(Received 19 May 2012; published 19 December 2012)

Above a critical chemistry-dependent molecular weight, all polymer molecules entangle and, as a result, exhibit slow dynamics, enhanced viscosity, and elasticity. Herein we report on the dynamics of low molecular weight polymers tethered to nanoparticles and find that even conventionally unentangled chains manifest dynamical features similar to entangled, long-chain molecules. Our findings are shown to imply that crowding and confinement of polymers on particles produce topological constraints analogous to those in entangled systems.

DOI: [10.1103/PhysRevLett.109.258301](https://doi.org/10.1103/PhysRevLett.109.258301)

PACS numbers: 47.57.Ng, 68.47.Pe, 82.35.Np, 83.80.-k

Transport properties of high molecular weight polymers generally differ from their low molecular weight counterparts, and this feature is commonly understood to arise from entanglement effects [1]. Entanglements are topological constraints imposed on a molecule by its neighbors, which limit its side-to-side motions to the region along the polymer contour [2–5]. Edwards [6] proposed the concept of a mean-field tube to model these constraints, and de Gennes introduced the idea of reptation to explain how topologically constrained molecules relax on long time scales [7]. High among the list of successes of the tube model is its ability to quantitatively predict dynamics of high molecular weight polymers with simple linear, as well as complex, branched, and ring, topologies [8–10]. There have also been several notable reports that offer “direct” evidence in support of the tube concept and for the molecular entanglements that produce it [11–13].

We have experimentally investigated the dielectric relaxation of low molecular-weight polymers tethered to inorganic nanoparticles. We find that in addition to the typical slowing down in relaxation expected from surface attachment and confinement of polymer chains [14–16], dynamics of the tethered polymers manifest similarities to those of entangled star polymer melts composed of long chains with orders of magnitude higher molecular weight.

Self-suspended nanoparticle suspensions [16,17] are used here as model systems for studying tethered polymer dynamics. Created by densely grafting polymer chains to nanoparticles [18], these suspensions are advantageous for studying surface dynamics because all polymer chains are anchored to nanoparticles. This makes it possible to use “bulk,” high signal-to-noise measurements to probe dynamics of single-molecule thick surface layers. Cis,1-4 polyisoprene (PI) is a *type-A* dielectric material [19]. PI has a net dipole moment parallel to its end-to-end vector. Broadband dielectric relaxation studies of bulk self-suspended nanoparticle suspensions based on PI therefore provide unique opportunities for investigating dynamics of tethered polymer chains.

Figure 1 compares the dielectric loss spectra,  $\varepsilon''(f)$ , for untethered PI of molecular weight 5000 g/mol and a self-suspended suspension composed of  $10 \pm 2$  nm silica particles grafted with the same polymer at a coverage of 1.5 chains/nm<sup>2</sup>. The measurements were performed using a Novocontrol broadband dielectric spectrometer with sandwich-type gold-plated copper fixtures. Several important features can be noted from the figure. A loss maximum is observed at low frequencies for both materials, and the positions of the maxima are shifted significantly to the left for the tethered polymer. Both the breadth and height of the  $\varepsilon''$  maxima are also seen to be larger for the tethered polymer. The relative dielectric strength,

$$\Delta\varepsilon = F \left( \frac{4\pi\mu}{3kT} \right) \nu R_e^2, \quad (1)$$

is evidently substantially greater for tethered polymers. Here  $R_e$  is the end-to-end distance and  $\nu$  the number density of polymer chains.  $\mu$  is the dipole moment per segment, and  $F$  is a correction factor [20,21]. From  $\Delta\varepsilon$  it is possible to determine  $R_e$  of the tethered PI to be around 9.3 nm, which is about 5 times larger than the random coil size,  $R_g$ , of the polymer. The tethered polymer chains are therefore stretched to form an extended brush on the particles. The nanoparticle separation corresponding to this volume fraction can be estimated as 22 nm, which implies that the polymer chains on adjacent particles are interdigitated.

Figure 2 shows the effect of grafting density  $\Sigma$  on the normal-mode relaxation time,  $\tau = (2\pi f_{\text{peak}})^{-1}$ ;  $f_{\text{peak}}$  is the frequency corresponding to the low-frequency maximum in  $\varepsilon''$ . It can be seen that for a range of temperatures,  $\tau$  for tethered PI is significantly larger than for the untethered polymer. The figure also reveals that the slowdown in molecular relaxation is unaffected by  $\Sigma$  or the particle volume fraction  $\varphi$ . Also, in the few cases where the high-frequency segmental modes are accessible in the dielectric spectra (see Supplemental Material [22]), we find that the large changes in  $\tau$  are accompanied by small or no changes in the segmental relaxation time.

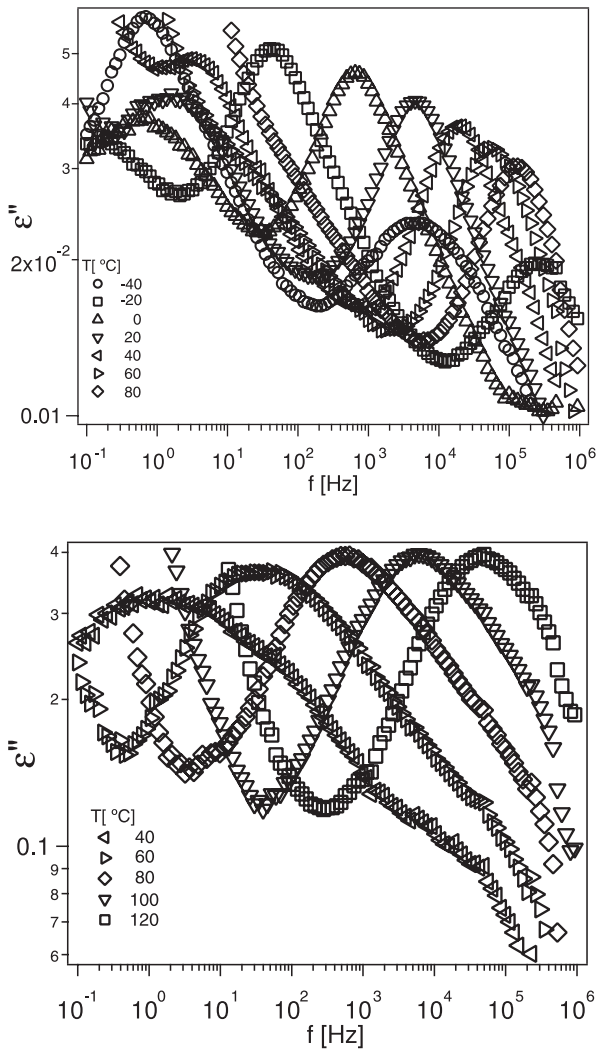


FIG. 1. Broadband dielectric loss  $\epsilon''$  spectra as follows: (a) Untethered polyisoprene with molecular weight ( $M_w$ ) of 5000 g/mol. The loss maximum at low frequency corresponds to the normal mode relaxation of the polymer chains. It is also evident that the position of the maximum shifts to higher frequency with increasing temperature, implying thermal speeding up of the polymer chain relaxation. (b) Nanoparticle tethered polyisoprene with molecular weight of 5000 g/mol. The volume fraction of silica nanoparticles in this sample is 10%.

Figure 3 shows the effect on dynamics of changing PI molecular weight. The volume fraction of silica nanoparticles are 11.1, 5.4, and 7.4%, respectively, for the three polymer molecular weights, 3000, 5000, and 15 000 g/mol. As expected,  $\tau$  for the untethered polymer increases with PI molecular weight [1–4]. In contrast, for tethered PI it shows no noticeable dependence, implying that the relative slowing down increases as molecular weight is lowered. Shorter chains therefore pay the highest penalty for being tethered to the nanoparticle surface. This finding is consistent with expectations from a recent density-functional theory for self-suspended suspensions

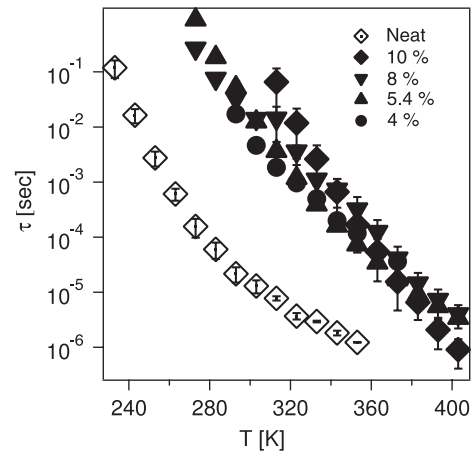


FIG. 2. Normal mode relaxation time as a function of temperature for untethered (open symbols) and tethered polyisoprene ( $M_w = 5000$  g/mol), at different nanoparticle volume fractions. Nanoparticle volume fraction is varied by changing the polymer grafting density.

and is considered to reflect greater difficulty for shorter chains to uniformly fill the interparticle space [17].

Previous studies of star-branched PI with molecular weights up to 20 kg/mole [23] reported that tethering slows down polymer relaxation by a factor of about 4, i.e., close to what is expected from a simple bead-spring, Rouse, model with the appropriate boundary conditions for a chain tethered at one end [24]. In contrast,  $\tau$  for particle-tethered PI are 2 to 3 orders of magnitude larger than for untethered polymers. For entangled star polymers it is known that  $\tau$  is exponentially larger and more broadly distributed than for the unlinked star arms. It is also essentially insensitive to the number of arms [4,25,26].

To make the analogy to entangled stars more concrete, we hypothesize that crowding and jostling of polymer chains tethered to nanoparticles can create entangled-polymer-like dynamics. The space between the grafted chains might then be imagined to play the role of a confining tube, and the surface spacing  $\xi$  defines an effective tube diameter. Typical values for  $\xi$  are given in Table I, where it is seen to be smaller than the random-walk step size (0.82 nm). This means that, ignoring the strong curvature of the particles, crowding on the particles would force PI chains to form an extended brush, in agreement with our earlier conclusion from the dielectric strength data.

Analogous to a chain in a tube, the crowded environment on the particle can be thought to restrict lateral movement of individual chains [see Fig. 4(a)]. As in the case of an entangled star polymer, relaxation requires the arm to retract down the tube and launch out in a new independent direction in order to explore a new configuration [Fig. 4(b)]. The end-to-end vector relaxation time for each arm can therefore be estimated as [25]

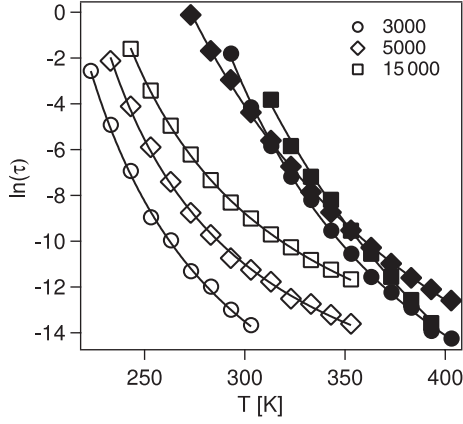


FIG. 3. Comparison of the relaxation time of nanoparticle tethered and untethered PI for different polymer molecular weight. Solid lines are fits with the Vogel-Fulcher-Tamman equation discussed in the Supplemental Material.

$$\tau: N^{5/2} \exp\left(\frac{\gamma' \langle L \rangle^2}{2R_g^2}\right), \quad (2)$$

where  $N$  is the number of entanglements per arm,  $\langle L \rangle$  is the contour length, and  $\gamma'$  is the effective spring constant. The brush height  $h$  plays the role of  $\langle L \rangle$ , and  $N \approx h^2/R_g^2$ , yielding

$$\tau: \left(\frac{h}{R_g}\right)^5 \exp\left(\frac{\gamma' h^2}{2R_g^2}\right). \quad (3)$$

The average relaxation time of the untethered chains scales as  $\tau_u \sim N_a^2$ , and the ratio of tethered and untethered polymer relaxation times can therefore be written as

$$\frac{\tau}{\tau_u} : \left(\frac{\Delta \varepsilon_t}{\Delta \varepsilon_u (1 - \varphi)}\right)^{5/2} \left[ \exp\left(\frac{\gamma' \Delta \varepsilon_t}{2\Delta \varepsilon_u (1 - \varphi)}\right) \right] / N_a^2, \quad (4)$$

where  $N_a$  is the number of segments in the arm.

Remarkably, this simple “entangled-star” model accounts for even subtle features of particle-tethered PI

TABLE I. Physical properties of self-suspended PI suspensions investigated by broadband dielectric relaxation spectroscopy.

$M_w^a$	$\varphi^b$ (%)	$R_g$	$N^c$	$\xi^d$
5000	10	2.23	614	0.404
5000	8	2.23	701	0.378
5000	5.4	2.23	1150	0.295
5000	4	2.23	1535	0.255
15 000	7.4	3.86	286	0.592
3000	11.1	1.72	1437	0.264

<sup>a</sup> $M_w$  is the molecular weight of the polymer.

<sup>b</sup> $\varphi$  is the volume fraction of silica nanoparticles.

<sup>c</sup> $n$  is the number of polymer chains attached to each nanoparticle.

<sup>d</sup> $\xi$  is the lateral spacing between the polymer chains.

relaxation. For instance, Eq. (4) yields  $\tau/\tau_u$  ratios of  $4 \times 10^4$ ,  $4.6 \times 10^3$ , and 1000, for PI with molecular weights of 3000, 5000, and 15 000 g/mol, respectively. These values are not only of the correct order of magnitude, but also follow the observed experimental trend. Additionally, in the range of grafting densities investigated,  $h$  is only a weak function of  $\Sigma$ , explaining the weak dependence of  $\tau$  on  $\Sigma$  or  $\varphi$  apparent in Fig. 3.

The solid lines in Fig. 3 are fits obtained using the Vogel-Fulcher-Tamman equation [24]:

$$\log(\tau) = A + \left(\frac{B}{T - C}\right). \quad (5)$$

Values of the fitting parameters for the untethered and tethered polymers are provided in Supplemental Material Tables 1 and 2. The activation energy  $B$  for the tethered PI is about 2–4 times the values for the untethered chains, with the largest increase seen for the highest molecular weight polymer. By comparison, they are reported to be nearly identical for entangled stars and for the unlinked arms. It is also apparent that contrary to results for small molecules confined in zeolites [27], no transition to single-molecule-like, Arrhenius, dynamics are observed, implying that the dominant effect that produces the slowdown in relaxation rate for particle-tethered PI is tethering.

In an entangled branched polymer melt, the final stress relaxation event is thought to be diffusion of the core or anchor point [28], which allows the retracted arms to explore all of the configuration space. Considering the large size of our nanoparticle anchors, the fact that there are hundreds of polymer chains tethered to each nanoparticle, and the highly crowded or jammed environment in which the particles must diffuse, this stage of stress relaxation is expected to be extraordinarily slow. This expectation is borne out nicely in frequency-dependent dynamic mechanical moduli for particle-tethered polymers of a wide range of chemistries and molecular weights (Supplementary Fig. S4 [22]). We therefore tentatively conclude that slow diffusion of the nanoparticles keeps

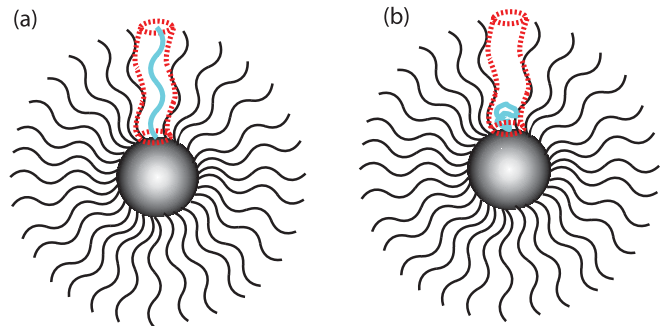


FIG. 4 (color). Schematic representation of the following: (a) Particle-tethered polymer chain confined in a tube owing to crowding by neighboring chains; (b) Arm retraction mechanism for the relaxation of the tethered polymer chain.

the tethered chains in long-lived frustrated states, as the “new” environment encountered after retraction is only marginally less constraining than the old. The higher activation energy is thought to reflect this frustration.

We close by noting that our findings are significantly different from previous reports of relaxation in polymer-nanoparticle composites. Ding *et al.* [29] studied the normal and segmental mode relaxation of polyisoprene- $C_{60}$  nanocomposites and found insignificant changes in normal mode time scales owing to the addition of  $C_{60}$  fillers to the PI matrix. Mijovic *et al.* [30] studied PI clay composites and reported that normal mode and segmental relaxation times remain unaffected by the addition of fillers for low and high molecular weight PI. But, for high molecular weight PI, the normal mode relaxation time increases with clay content. Our findings are also quite different from observations reported by Kremer and co-workers [27] for confinement dynamics of small molecule liquids, where a transition to faster, single-molecule dynamics is observed upon confinement. We conclude that the dominant effect responsible for the behaviors seen for nanoparticle-tethered PI are a consequence of the end attachment of the polymer chains to slow-moving or jammed particles [31].

In conclusion, we have discovered that low molecular weight polymers densely grafted to nanoparticles manifest unusual, slow dynamics reminiscent of high molar mass entangled polymers. We show that a simple arm retraction model for entangled star polymers can explain many of our observations. Our findings also imply that molecular dynamics previously attributed to tube-like confinement in high molecular weight polymers can be engineered even in low molecular weight molecules through surface crowding and confinement.

This work was supported by the National Science Foundation Grant No. DMR-1006323 and by Grant No. KUS-C1-018-02, made by King Abdullah University of Science and Technology (KAUST). Facilities available though the Cornell Center for Materials Research (CCMR) were used for this study.

- 
- [1] G. C. Berry and T. G. Fox, *Adv. Polym. Sci.* **5/3**, 161 (1968).
  - [2] W. W. Graessley, *Adv. Polym. Sci.* **47**, 67 (1974).
  - [3] M. Doi and S. F. Edwards, *Theory of Polymer Dynamics* (Oxford University Press, New York, 1988).
  - [4] M. Rubinstein and R. H. Colby, *Polymer Physics* (Oxford University Press, New York, 2003).
  - [5] T. C. B. Mcleish, *Adv. Phys.* **51**, 1379 (2002).
  - [6] S. F. Edwards and J. J. Grant, *J. Phys. A* **6**, 1169 (1973).

- [7] P. G. de Gennes, *J. Chem. Phys.* **55**, 572 (1971).
- [8] M. Kapnistos, M. Lang, D. Vlassopoulos, W. Pyckhout-Hintzen, D. Richter, D. Cho, T. Chang, and M. Rubinstein, *Nat. Mater.* **7**, 997 (2008).
- [9] T. C. B. Mcleish, *Science* **297**, 2005 (2002).
- [10] D. J. Read, D. Auhl, C. Das, J. den Doelder, M. Kapnistos, I. Vittorias, and T. C. B. McLeish, *Science* **333**, 1871 (2011).
- [11] J. Klien, *Nature (London)* **271**, 143 (1978).
- [12] J. Kas, H. Strey, and E. Sackman, *Nature (London)* **368**, 226 (1994).
- [13] T. T. Perkins, D. E. Smith, and S. Chu, *Science* **264**, 819 (1994).
- [14] N. W. Hu and S. Granick, *Science* **258**, 1339 (1992); Y. K. Cho, H. Watanabe, and S. Granick, *J. Chem. Phys.* **110**, 9688 (1999).
- [15] Q. Zhang and L. A. Archer, *Langmuir* **19**, 8094 (2003); T. T. Dao and L. A. Archer, *Langmuir* **17**, 4042 (2001).
- [16] P. Agarwal, H. Qi, and L. A. Archer, *Nano Lett.* **10**, 111 (2010); P. Agarwal and L. A. Archer, *Phys. Rev. E* **83**, 041402 (2011).
- [17] H. Y. Yu and D. L. Koch, *Langmuir* **26**, 16 801 (2010).
- [18] A. B. Bourlinos, R. Herrera, N. Chalkias, D. D. Jiang, Q. Zhang, L. A. Archer, and E. P. Giannelis, *Adv. Mater.* **17**, 234 (2005); R. Rodriguez, R. Herrera, L. A. Archer, and E. P. Giannelis, *Adv. Mater.* **20**, 4353 (2008).
- [19] M. E. Baur and W. H. Stockmayer, *J. Chem. Phys.* **43**, 4319 (1965).
- [20] K. Adachi and T. Kotaka, *Prog. Polym. Sci.* **18**, 585 (1993).
- [21] H. Watanabe, *Macromol. Rapid Commun.* **22**, 127 (2001).
- [22] See Supplemental Material at <http://link.aps.org/supplemental/10.1103/PhysRevLett.109.258301> for the data on the segmental mode relaxation and rheology of the systems studied.
- [23] D. Boese, F. Kremer, and L. J. Fetters, *Macromolecules* **23**, 1826 (1990).
- [24] W. W. Graessley, *Adv. Polym. Sci.* **47**, 67 (1982).
- [25] L. J. Fetters, A. D. Kiss, D. S. Pearson, G. F. Quack, and F. J. Vitus, *Macromolecules* **26**, 647 (1993).
- [26] Y. Matsumiya and H. Watanabe, *Macromolecules* **34**, 5702 (2001).
- [27] A. Huwe, F. Kremer, P. Behrens, and W. Schwieger, *Phys. Rev. Lett.* **82**, 2338 (1999).
- [28] J. H. Lee, L. J. Fetters, and L. A. Archer, *Macromolecules* **38**, 10 763 (2005).
- [29] Y. Ding, S. Pawlus, A. P. Sokolov, J. F. Douglas, A. Karim, and C. L. Soles, *Macromolecules* **42**, 3201 (2009).
- [30] J. Mijovic, H. Lee, J. Kenny, and J. Mays, *Macromolecules* **39**, 2172 (2006).
- [31] P. Agarwal, S. Srivastava, and L. A. Archer, *Phys. Rev. Lett.* **107**, 268302 (2011).